Quality Factors in Micron- and Submicron-Thick Cantilevers

Kevin Y. Yasumura, Timothy D. Stowe, Eugene M. Chow, Timothy Pfafman, Thomas W. Kenny, Barry C. Stipe, and Daniel Rugar, *Member, IEEE*

***Abstract*—Micromechanical cantilevers are commonly used for detection of small forces in microelectromechanical sensors (e.g., accelerometers) and in scientific instruments (e.g., atomic force microscopes). A fundamental limit to the detection of small forces is imposed by thermomechanical noise, the mechanical analog of Johnson noise, which is governed by dissipation of mechanical energy. This paper reports on measurements of the mechanical quality factor Q for arrays of silicon–nitride, polysilicon, and single-crystal silicon cantilevers. By studying the dependence of Q on cantilever material, geometry, and surface treatments, significant insight into dissipation mechanisms has been obtained. For submicron-thick cantilevers, Q is found to decrease with decreasing cantilever thickness, indicating surface loss mechanisms. For single-crystal silicon cantilevers, significant increase in room temperature Q is obtained after 700 °C heat treatment in either N_2 or forming gas. At low temperatures, silicon cantilevers exhibit a minimum in Q at approximately 135K, possibly due to a surface-related relaxation process. Thermoelastic dissipation is not a factor for submicron-thick cantilevers, but is shown to be significant for silicon–nitride cantilevers as thin as 2.3 μm. [434]**

***Index Terms*—Cantilever, force sensor, mechanical dissipation, micromechanical resonator, quality factor, surface losses.**

I. Introduction

THE majority of microfabricated sensors measure forces applied to micromechanical flexures. Examples include pressure sensors, which measure force on a diaphragm, and accelerometers, which measure inertial force on a proof mass. Many of these microfabricated sensors are capable of measuring surprisingly small forces. For example, the Analog Devices ADXL05 accelerometer features a proof mass of approximately 10^{-10} kg and is capable of detecting an acceleration as small as 5×10^{-4} times the acceleration of gravity in a 1-Hz bandwidth.[1] This acceleration represents a force of 0.5 pN applied to the mass.

Manuscript received March 26, 1999; revised November 12, 1999. An earlier version of this paper was presented at the 1998 Tranducers Research Foundation Hilton Head Workshop. This work was supported by the National Science Foundation under CAREER Award ECS-9502046, by the National Science Foundation under GOALI Award ECS-9422255, by the National Science Foundation Instrumentation for Materials Research Program under Contract DMR 9504099, under a Terman Fellowship, and by the Office of Naval Research under Contract N00014-98-C-0070. Subject Editor, W. N. Sharpe, Jr.

K. Y. Yasumura, T. D. Stowe, E. M. Chow, and T. W. Kenny are with the Departments of Applied Physics, Electrical Engineering, and Mechanical Engineering, Stanford University, Stanford, CA 94305-4021 USA (e-mail kevin@micromachine.stanford.edu).

T. Pfafman was with the Department of Mechanical Engineering, Stanford University, Stanford, CA 94305-4021 USA. He is consulting in the Bay area.

B. C. Stipe and D. Rugar are with the IBM Research Division, Almaden Research Center, San Jose, CA 95120-6099 USA.

Publisher Item Identifier S 1057-7157(00)02134-X.

Ordinarily, sensor performance is improved by reducing the noise of the preamplifier used to convert the physical signals to electrical signals, and by controlling other error sources such as uncompensated thermal drift. There eventually comes a point, however, where thermodynamics imposes a barrier to further sensor improvement. For the case of microcantilevers optimized for use in force detection, thermomechanical noise sets a limit to the ultimate force resolution [1].

Thermomechanical noise is a consequence of the cantilever being in thermal equilibrium with its environment (i.e., a heat bath with many microscopic degrees of freedom). Energy dissipation in the cantilever causes the stored mechanical energy to leak away and be converted into heat. The stronger the coupling between the cantilever and heat bath, the faster the decay of cantilever motion toward thermal equilibrium and the lower the mechanical quality factor Q of the oscillating mode. Conversely, the coupling to the heat bath has the consequence that the cantilever will be subjected to constant random excitation by its interaction with the many microscopic degrees of freedom in the heat bath. This relationship between the energy dissipation and random thermal excitation is embodied in the "fluctuation–dissipation theorem" of statistical mechanics, which applies to mechanical systems just as it applies to the Johnson noise across an electrical resistor [2, pp. 572–573]. The net result is that the lower the mechanical Q of the system, the larger the force noise.

The equipartition theorem gives a measure of how much thermal energy is in each mode of a microcantilever [2, pp. 248–249]. The mean square vibration amplitude associated with a mode of oscillation at temperature T is given by

$$\frac{1}{2}k_B T = \frac{1}{2}k\langle x^2\rangle \tag{1}$$

where k is the cantilever spring constant and x is the cantilever displacement. We can calculate the equivalent force noise associated with mechanical dissipation by assuming that the cantilever behaves as a simple harmonic oscillator and imposing the requirement that random thermal excitations must produce the mean square vibration amplitude given by (1). The mean square vibration amplitude is the integral over all frequencies of the force noise spectral density multiplied by the square of the mechanical transfer function

$$\langle x^2\rangle = \int_0^\infty |G(f)|^2 S_F \, df \tag{2}$$

[1]Analog devices technical data sheet for ADXL05 single-chip accelerometer with signal conditioning

where the transfer function is

$$G(f) = \frac{f_0^2/k}{(f_0^2 - f^2) + i(ff_0/Q)}. \tag{3}$$

With the assumption that the force noise spectrum is white (i.e., frequency independent), (1)–(3) lead to a spectral density of $S_F = 4kk_BT/\omega_0 Q$, where $\omega_0 = 2\pi f_0$ is the cantilever resonance frequency. This spectral density results in a force noise in a bandwidth B of

$$F_{\min} = \sqrt{\frac{4kk_BTB}{\omega_0 Q}}. \tag{4}$$

For a simple rectangular cantilever, this minimum detectable force can also be expressed in terms of the cantilever dimensions

$$F_{\min} = \left(\frac{wt^2}{lQ}\right)^{1/2} (k_BTB)^{1/2}(E\rho)^{1/4} \tag{5}$$

where E is the Young's ρ is the mass density of the cantilever material, w is the cantilever width, l is the cantilever length, and t is the cantilever thickness.

From (5), for the minimum detectable force, a strategy can be found to design ultrasensitive cantilevers: make them narrow, thin, and long. This strategy is effective only if high mechanical Q is maintained. Unfortunately, relatively little is understood about the mechanisms responsible for energy dissipation in micron- and submicron-thick microstructures. To better understand the dissipation mechanisms, we have studied cantilever Q factor as a function of controllable cantilever properties such as material, geometry, and surface treatment. In this paper, we present the results from this ongoing study.

II. Loss Mechanisms

For a cantilever operating in vacuum, vibrational energy can be dissipated via coupling to the support structure (clamping loss) and by internal friction. Internal friction results from a variety of physical mechanisms, including motion of lattice defects, thermoelastic dissipation (TED), phonon–phonon scattering, etc. [3]. Traditionally, internal friction is considered as a bulk (volume) effect, but surface effects can dominate for submicron-thick cantilevers or for resonators with very high Q [4], [5].

Cantilever Q is defined as $Q = 2\pi W_0/\Delta W$, where W_0 is the stored vibrational energy and ΔW is the total energy lost per cycle of vibration. Since ΔW can be written as $\Delta W = \sum_i \Delta W_i$, where ΔW_i represents the energy lost due to the various dissipation mechanisms, we can write the inverse Q as the sum

$$\begin{aligned}\frac{1}{Q} &= \sum_i \frac{1}{Q_i} \\ &= \frac{1}{Q_{\text{clamping}}} + \frac{1}{Q_{\text{TED}}} + \frac{1}{Q_{\text{volume}}} + \frac{1}{Q_{\text{surface}}} + \frac{1}{Q_{\text{other}}}\end{aligned} \tag{6}$$

where we have explicitly included terms to characterize clamping loss, TED, bulk internal friction (other than TED), and surface effects.

Clamping loss was studied theoretically by Jimbo and Itao [6], [7] using a two-dimensional theory that modeled the support structure as an infinitely large elastic body. Their calculations result in the estimate $Q_{\text{clamping}} \approx 2.17\ l^3/t^3$. For all of the cantilevers studied here, $l/t > 39$, giving $Q_{\text{clamping}} > 1.3 \times 10^5$. Since this is significantly larger than any of our measured Q values, we conclude that clamping loss does not limit Q for our structures.

The effect of TED will be considered in detail in Section VII. In general, for submicron-thick cantilevers operating at kilohertz frequencies, TED is negligible. However, as we shall discuss later, TED can become the dominant source of energy dissipation in thicker silicon–nitride cantilevers.

In order to better understand the effect of internal friction and the relative importance of volume and surface contributions, we now consider a simple model of a vibrating cantilever where we treat the stress and strain in the cantilever as scalars (ignoring tensor properties) and assume that the cantilever vibration amplitude is small compared to the length of the cantilever. The energy dissipation is modeled by considering a complex-valued Young's modulus $E = E_1 + iE_2$, where E_1 is the conventional (real-valued) Young's modulus and E_2 is the dissipative part, which we will assume to be small compared to E_1. For dissipative processes that occur on the atomic scale (such as motion of lattice defects), E_2 can be considered to be a property of the material and its defects, though it may have substantial frequency and temperature dependence depending on the types of processes involved. For more macroscopic processes, such as TED, E_2 can also have explicit dependence on cantilever geometry.

For a cantilever vibrating sinusoidally such that the strain is given by $\varepsilon(\boldsymbol{r}, \tau) = \varepsilon_m(\boldsymbol{r}) \sin \omega\tau$, where τ is time, the stored energy can be written in terms of the peak elastic energy [8]

$$W_0 = \int_V dV \int_0^{\varepsilon_m} \sigma\, d\varepsilon = \frac{1}{2} \int_V E_1 \varepsilon_m^2(\boldsymbol{r})\, dV \tag{7}$$

where σ is the longitudinal stress and $\varepsilon_m(\mathbf{r})$ is the peak strain. For a simple rectangular cantilever, the volume integral is over the cantilever thickness ($z = -t/2$ to $z = +t/2$), width ($y = -w/2$ to $y = +w/2$), and length ($x = 0$ to $x = l$).

The exact form of $\varepsilon_m(\boldsymbol{r})$ depends on the cantilever geometry and vibrational mode shape. For a cantilever with rectangular cross section, the strain is uniform across the width of the cantilever and increases linearly in z away from the neutral plane ($z = 0$). Accordingly, we write

$$\varepsilon_m(\boldsymbol{r}) = \frac{2z}{t}\, \varepsilon_{\max}(x) \tag{8}$$

where $\varepsilon_{\max}(x)$ is the strain that occurs along the top surface of the cantilever (where the strain is maximum). This expression holds even for higher order vibrational modes of a rectangular cantilever. Combining (7) and (8) gives

$$W_0 = \frac{1}{6}\, wtE_1 \int_0^l \varepsilon_{\max}^2(x)\, dx. \tag{9}$$

Now consider energy dissipation. For a bulk (volume) loss mechanism, the energy lost per cycle can be written as [8]

$$\Delta W_V = \int_V dV \oint \sigma \, d\varepsilon = \pi \int_V E_2 \varepsilon_m^2(\boldsymbol{r}) \, dV. \tag{10}$$

Here, $\oint$ signifies integration over a complete cycle of vibration. Note that if E_1 and E_2 are constants (as they would be for a cantilever made of a single material), the volume integrals on the right-hand sides of (7) and (10) differ only by a constant factor. Thus, the Q factor is independent of cantilever geometry and vibrational mode shape and is given by

$$Q_{\text{volume}} = \frac{E_1}{E_2}. \tag{11}$$

Next consider the effect of a thin surface layer that exhibits enhanced dissipation. The dissipation enhancement may be due to the disruption of the atomic lattice at the surface or due to a thin layer of surface contamination. In most cases, the surface layer will not substantially change the stored energy in the cantilever, but it can significantly enhance the dissipated energy. Characterizing the surface layer by thickness δ and complex modulus $E^S = E_1^S + iE_2^S$, the energy lost per cycle due to the surface layer is

$$\Delta W_S = \pi \int_V E_2^S \, \varepsilon_m^2(\boldsymbol{r}) \, dV \tag{12}$$

where the volume of integration is confined to the surface layer, which we assume to be on the top, bottom, and sides of the cantilever. If δ is small compared to the dimensions of the cantilever, (12) can be converted to a sum of surface integrals and then evaluated using (8) to yield

$$\Delta W_S = 2\pi\delta E_2^S \left(w + \frac{t}{3}\right) \int_0^l \varepsilon_{\max}^2(x) \, dx. \tag{13}$$

Using (9) and (13) to evaluate the Q factor, we obtain

$$Q_{\text{surface}} = \frac{wt}{2\delta(3w+t)} \frac{E_1}{E_2^S}. \tag{14}$$

If we define the Q factor of the material that comprises the surface layer as $Q_S = E_1^S/E_2^S$, then (14) may be rewritten as

$$Q_{\text{surface}} = \frac{wt}{2\delta(3w+t)} \frac{E_1}{E_1^S} Q_S. \tag{15}$$

For a thin wide cantilever where $t \ll w$, Q_{surface} is proportional to cantilever thickness and given by

$$Q_{\text{surface}} = \frac{t}{6\delta} \frac{E_1}{E_1^S} Q_S. \tag{16}$$

Based on the results in (15) and (16), we would, therefore, expect to see a strong thickness dependence to the cantilever Q factor should the dominant loss mechanism be surface related.

III. Cantilever Fabrication

Three materials have been used to fabricate our cantilevers—silicon nitride, polysilicon, and single-crystal silicon. The first, silicon nitride, was chosen because of its durability, ease of fabrication, and general use as a processing material. The second material, polysilicon, was chosen because of its wide use as a micromechanical sensor material. A number of fabrication processes rely on a top polysilicon layer from which a sensor or device is fabricated, making a study of dissipation in polysilicon resonators of wide interest. The last material, single-crystal silicon, was chosen because of its expected low internal friction as exhibited by larger bulk oscillators [3], [9] and low internal stress, allowing for the fabrication of ultrathin cantilevers with little or no curling [10].

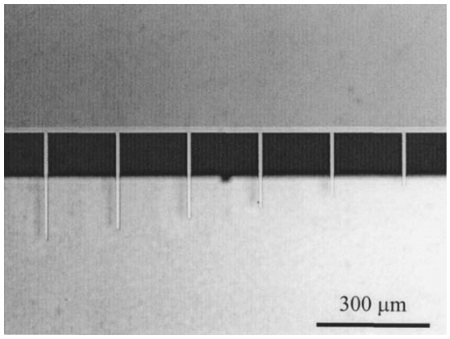

Fig. 1. Array of 2000-Å-thick silicon–nitride cantilevers. Shown is part of an array of $w = 10$ μm cantilevers of length varying from 150 to 300 μm. Cantilever arrays made from silicon nitride and polysilicon use this array pattern.

Silicon–nitride cantilevers, as shown in Fig. 1, were fabricated from low-stress silicon nitride grown using low-pressure chemical vapor deposition on $\langle 100 \rangle$ silicon wafers. After film deposition, the cantilevers were patterned by photolithography and then defined using an SF_6 dry etch. Tetramethylammonium hydroxide (TMAH) was then used to etch away the exposed silicon and undercut the cantilevers, thereby releasing them. After rinsing in water and methanol, the cantilevers were dried using a CO_2 critical point drier [11].

Polysilicon cantilevers were fabricated from polysilicon-on-insulator wafers. Starting with a $\langle 100 \rangle$ silicon wafer, a 4000-Å-thick layer of thermal oxide was grown. Next, a polysilicon layer of the desired thickness was deposited and cantilevers were etched using an SF_6 plasma etch. Protective layers of low-temperature oxide and silicon nitride were then deposited to protect the cantilevers during subsequent backside patterning and a TMAH etch. The topside silicon nitride layer was then removed and a buffered oxide etch (BOE) was used to free the oxide-encased cantilever structures. Finally, a critical point drying step was performed.

Single-crystal silicon cantilevers start with $\langle 100 \rangle$ silicon-on-insulator wafers. A thermal oxidation was performed to thin down the top silicon layer to the desired cantilever thickness. BOE was then used to remove the top oxide layer exposing the top silicon layer for cantilever patterning. As in the polysilicon process, low-temperature oxide and silicon–nitride were deposited for frontside protection and as a backside masking layer during the backside TMAH etch. The cantilevers were then released with BOE followed by critical point drying. Fig. 2 shows an array of 1700-Å-thick single-crystal silicon cantilevers. Further details of the fabrication process can be found in the work of Stowe *et al.* [10].

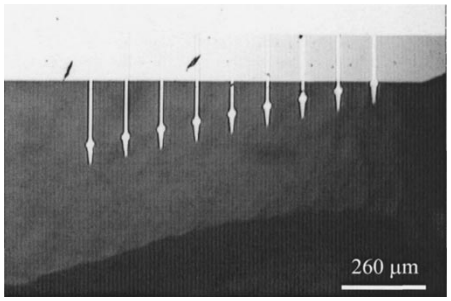

Fig. 2. Array of 1700-Å-thick single-crystal silicon cantilevers. The cantilevers have necks of width 5 μm and lengths from 80 to 260 μm.

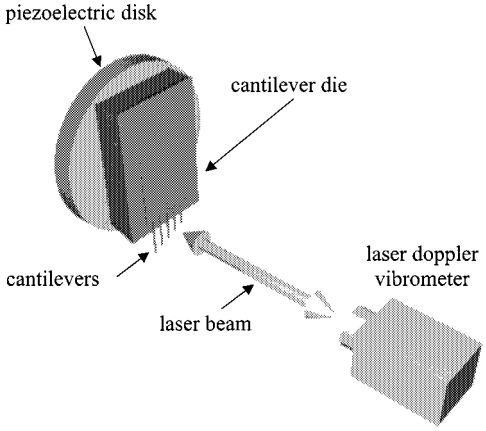

Fig. 3. Diagram of the room-temperature Q measurement system. Shown are the piezoelectric disk, cantilever die, and laser doppler vibrometer. Not shown is a viewport through which the incident laser passes through before striking the target cantilevers. The objects in this diagram are not to scale.

IV. Q Measurements

Unless otherwise specified, all measurements were performed at room temperature. A diagram of the experimental system used for room-temperature measurements is shown in Fig. 3. The cantilevers were placed in a vacuum chamber on a stack of piezoelectric disks. A viewport on the side of the chamber allows the use of an external laser doppler vibrometer to measure the cantilever motion. The laser doppler vibrometer is a commercially available system which measures the velocity-dependent doppler shift of the reflected laser radiation.[2] Low-temperature measurements were performed in a separate apparatus that uses a fiber-optic interferometer detection system.

A "free ring-down" technique was used to measure cantilever Q. The cantilevers were first driven on-resonance to a steady-state amplitude. The drive excitation was produced by applying an oscillating voltage to the piezoelectric disks on which the cantilever die was mounted. The drive was stopped abruptly and the cantilever motion was measured as the amplitude decayed. The ring-down was then fit to an exponential function. From the fit, the $1/e$ decay time constant of the ring-down τ_0 was obtained. The decay time constant allows calculation of the cantilever Q according to $Q = \pi\tau_0 f_0$. The quality of the exponential fit to the decay data allows us to be sure of the accuracy of each Q measurement. The data presented in this paper, unless otherwise indicated, are averages of multiple ring-down measurements for each cantilever. The error for each individual cantilever ring-down measurement is on the order of a few percent.

[2]302 sensor head with OVF3001 controller, Polytec P.I., Costa Mesa, CA.

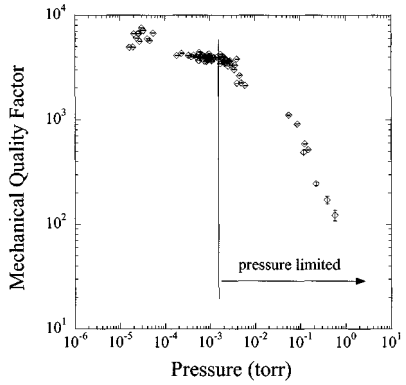

Fig. 4. Mechanical Q factor versus pressure for a 5100-Å-thick silicon–nitride cantilever. Above $\sim$1 mtorr, the Q is pressure limited. Below this pressure, the Q is limited by intrinsic dissipation mechanisms.

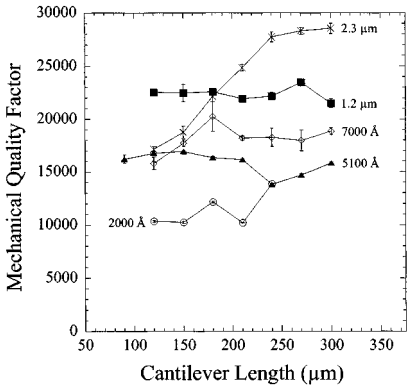

Fig. 5. Mechanical Q factor versus cantilever length for silicon–nitride cantilevers of thickness 2000, 5100, 7000 Å, 1.2 and 2.3 μm. Cantilever width is 10 μm for all five thicknesses.

One important source of energy dissipation in micromechanical oscillators is air damping. Fig. 4 shows a plot of Q versus pressure for a 5100-Å-thick silicon–nitride cantilever. For this cantilever, we can see that the Q is pressure limited above a pressure of approximately 1 mtorr. Below 1 mtorr, the dissipation associated with air damping becomes negligible compared to intrinsic loss mechanisms. The work described in this paper was performed under vacuum at a pressure of 10^{-6} torr. This is below the pressure limited transition point for the cantilevers studied.

In order to test the repeatability and long-term stability of a cantilever's Q, the Q was measured for a polysilicon cantilever ($t = 2.3$ μm, $w = 25$ μm, and $l = 210$ μm) over a period of 2 h. Over this 2-h time span the Q had a standard deviation of 1%, demonstrating excellent measurement reproducibility. On the other hand, after exposure to laboratory air for several days, cantilever Q's can change by 10% or more, depending on the cantilever thickness. Presumably, these changes are due to oxidation and contamination of the cantilever surface.

Measurements of Q for arrays of silicon–nitride cantilevers were carried out for thicknesses of 2000, 5100, 7000 Å, 1.2 and 2.3 μm, lengths from 90 to 300 μm, and widths of 5, 10, 25, and 50 μm. Fig. 5 shows the data for the 10-μm-wide cantilevers.

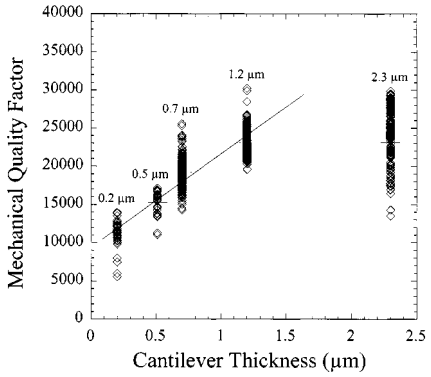

Fig. 6. Mechanical Q factor versus cantilever thickness for five silicon–nitride cantilever thicknesses (2000, 5100, 7000 Å, 1.2 and 2.3 μm). Each of the five clusters of points represents hundreds of individual Q measurements.

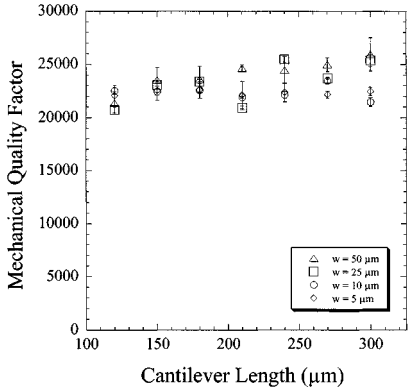

Fig. 7. Mechanical Q factor versus cantilever length for silicon–nitride cantilevers of thickness 1.2 μm. Cantilevers of widths 5, 10, 25, and 50 μm are shown.

Several trends are clear from this data. First, the Q is roughly independent of the cantilever length for all of the thicknesses, except the 2.3-μm-thick cantilevers. Both bulk (volume) and surface-dependent dissipative processes are expected to produce length independent Q's. The lower Q for the shortest of the 2.3-μm-thick cantilevers is believed to be caused by TED and will be discussed in greater detail later in this paper.

Fig. 6 shows a plot of cantilever Q versus cantilever thickness. In Fig. 6, there is an increase in the mechanical Q as the thickness of the cantilever increases. A linear fit to the four thinnest cantilever thicknesses is shown. For the four thinnest cantilever thicknesses, the strong thickness dependence is indicative of surface loss mechanisms, as discussed earlier.

Fig. 7 shows data for silicon–nitride cantilevers of thickness 1.2 μm. The cantilever widths are 5, 10, 25, and 50 μm. The Q's of these cantilevers are independent of the cantilever width. Just as the cantilever Q is expected to be length independent for both volume and surface dissipative processes, the cantilever Q should also be independent of cantilever width when $w \gg t$ [see (16)].

Single-crystal silicon cantilevers show geometrical dependence similar to the silicon–nitride devices. Fig. 8 shows data for single-crystal silicon cantilevers of thickness 600, 1700, and 2400 Å. Consistent with the data in Figs. 5 and 6, we see that the Q is roughly independent of cantilever length and increases with increasing cantilever thickness.

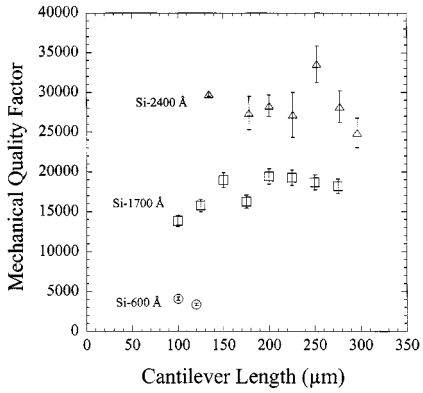

Fig. 8. Mechanical Q factor versus cantilever length for single-crystal silicon cantilevers of thickness 600, 1700, and 2400 Å.

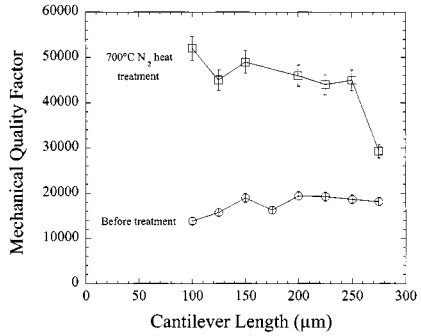

Fig. 9. Mechanical Q factor versus cantilever length for a die of 1700-Å-thick single-crystal silicon cantilevers showing the effect of heat treatment.

V. Heat Treatment

As seen in Figs. 6 and 8, the mechanical Q's of both silicon–nitride and single-crystal silicon cantilevers depend on cantilever thickness, suggesting surface-dominated dissipation mechanisms. Possible sources of surface dissipation are adsorbates on the cantilever surface or surface defects created during the cantilever fabrication process. Both of these sources might be expected to respond to heat treatment. To test this hypothesis, 1700-Å-thick single-crystal silicon cantilevers were heated for 1 h at 700 °C in a nitrogen atmosphere. As shown in Fig. 9, the Q increased by about a factor of three. In addition, 1-h heat treatment in 700 °C forming gas (Ar with 4.25% H_2) produced consistent factor of two increases in Q for 700-Å-thick silicon cantilevers.

VI. Low-Temperature Behavior

Low-temperature behavior of microcantilevers is of interest in experiments designed to achieve the lowest possible force noise. Fig. 10 is a plot of Q versus temperature for a heat-treated 700-Å- thick single-crystal silicon cantilever with a resonance frequency of 3.8 kHz and spring constant of 4×10^{-5} N/m. The room temperature Q of this cantilever was approximately 1×10^4. Upon cooling, the cantilever Q first decreases, reaching a broad minimum of 4×10^3 centered at approximately 135 K. By 77 K, the Q recovers its room temperature value and then increases rapidly as the temperature is lowered further. At 4 K, the Q reaches 2.5×10^4, roughly 2.5 times

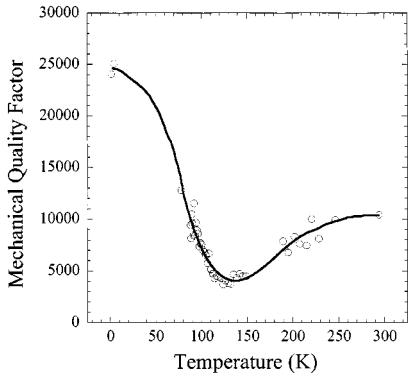

Fig. 10. Mechanical Q factor versus temperature for a $t = 700$ Å, $l = 144$ μm, and $w = 7$ μm single-crystal silicon cantilever. The resonance frequency of this cantilever was 3.8 kHz. The solid curve is meant as a guide to the eye.

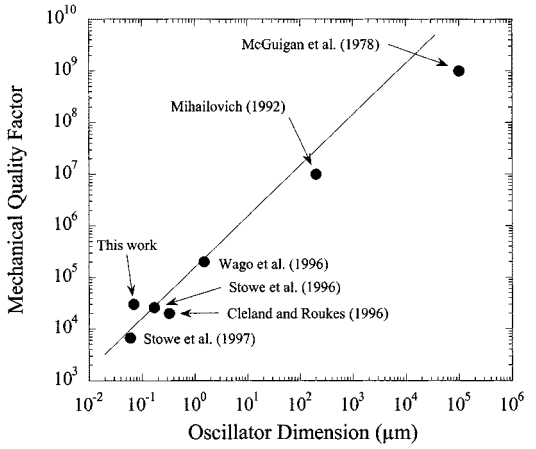

Fig. 11. Mechanical Q factor versus oscillator thickness for single-crystal silicon oscillators at $T = 4$K. Line fit is to the five thinnest oscillators.

the room-temperature value. Similar data was obtained for nonheat-treated cantilevers. Even though the room temperature Q's of heat-treated cantilevers were a factor of two larger than for nonheat-treated cantilevers, both heat- and nonheat-treated cantilevers had comparable Q's at 4 K.

Similar Q minima have been observed in all of our silicon microcantilevers, both heat treated and nonheat treated, and in micron-thick commercial silicon cantilevers. Previous studies on large single crystals of silicon have reported internal friction peaks in the range of 115–124 K [12], [13]. Since our observed dissipation peak is centered at higher temperature and is somewhat broader than that found in the bulk studies, it is likely to have a different origin. Some type of relaxation process related to surface imperfections, oxidation, or adsorbed contaminants is a possible cause.

Although the low temperature Q of the 700-Å-thick cantilever in Fig. 10 reaches 25 000 at 4 K, it is still significantly lower than has been observed in larger silicon oscillators. Fig. 11 shows a compilation of data from our work and from the literature at 4 K. As in the case of silicon–nitride cantilevers, the Q of single-crystal silicon oscillators is highly dependent on the oscillator thickness, suggesting surface-dominated loss mechanisms. Since this plot has data for different kinds of oscillators, it should not be over interpreted, but the general trend is evident—an increase in the mechanical Q as the oscillator dimensions increase. Included in Fig. 11 is data for ultrathin silicon cantilevers [10], [14], doubly supported high-frequency silicon resonators [15], commercially available silicon cantilevers [16], double torsional oscillators [17], and suspended bulk silicon crystals [12]. Shown in Fig. 11 is a line fit to the five thinnest oscillators ($t = 600$, 700, 1700, 3300 Å, and 1.5 μm). These micron- and submicron-scale oscillators have a roughly linear Q versus t dependence. The larger oscillators deviate from this linear dependence possibly because loss mechanisms other than surface mechanisms begin to dominate and limit the Q as the oscillator size increases.

VII. TED

Another possible source of energy loss in cantilever microstructures is TED [18], [19]. Thermoelastic energy dissipation is caused by irreversible heat flow across the thickness of the cantilever as it oscillates. The rate of energy dissipation due to this heat flow is dependent upon the cantilever geometry, material, and temperature. Roszhart [20] has shown that TED can be a dominant source of energy loss in single-crystal silicon cantilevers as thin as 10 μm. Although TED generally becomes less important as thickness is reduced, we show below that it can be significant in silicon–nitride cantilevers as thin as 2.3 μm.

If a load is applied to a cantilever that causes it to deflect in a flexural mode (a mode that entails localized volume changes), the regions under compression will warm while the regions under expansion will cool. This process creates a temperature gradient within the cantilever. Energy will then flow from the warmer regions to the cooler regions, resulting in an irreversible energy loss. The rate of energy loss depends upon the material properties: thermal conductivity, coefficient of thermal expansion, and heat capacity. It will also depend upon the resonance frequency of the oscillation mode and the thermal time constant for heat transfer from the warmer regions of the cantilever to the cooler regions. Following Roszhart [20], the thermoelastically limited Q factor Q_{TED} can be expressed as

$$Q_{\mathrm{TED}} = \frac{1}{2\Gamma(T)\Omega(f)}. \tag{17}$$

The term

$$\Gamma(T) = \frac{\alpha^2 TE}{4\rho C_p} \tag{18}$$

contains the material dependencies of the TED process: the coefficient of thermal expansion α, the cantilever temperature T, modulus of elasticity E, mass density ρ, and specific heat C_p. The other term

$$\Omega(f) = \frac{2f/F_0}{1 + (f/F_0)^2} \tag{19}$$

depends on the ratio of the cantilever frequency f to a characteristic frequency F_0, which quantifies the rate of heat flow across

TABLE I
MATERIAL CONSTANTS FOR SILICON NITRIDE AND SINGLE-CRYSTAL SILICON* [21]–[26]

Parameter	Silicon Nitride	Silicon	Units
α	3.0×10^{-6}	2.6×10^{-6}	K^{-1}
E	126×10^{9}	190×10^{9}	$N\text{-}m^{-2}$
ρ	3.44×10^{3}	2.33×10^{3}	$kg\text{-}m^{-3}$
C_p	0.71×10^{3}	0.70×10^{3}	$J\text{-}kg^{-1}\text{-}K^{-1}$
κ	3.2	1.5×10^{2}	$W\text{-}m^{-1}\text{-}K^{-1}$

*The modulus of elasticity for silicon nitride was determined from a curve fit of f versus l for an array of 2.3-μm-thick ($w = 10$ μm) cantilevers. For simple beam cantilevers oscillating in a flexural mode, $f \propto \sqrt{E}/l^2$. Curve fitting gave a value of $126 \pm 7 \times 10^9 \mathrm{N \cdot m^{-2}}$ for the modulus of elasticity.

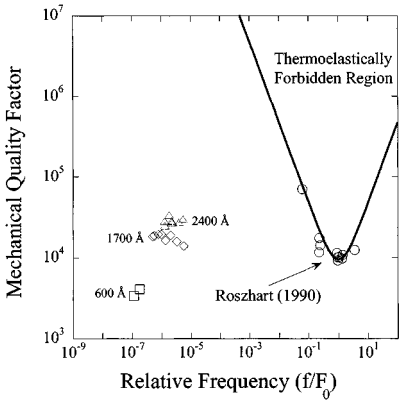

Fig. 12. Plot showing Q values for 600-, 1700-, and 2400-Å-thick silicon cantilevers. Also shown are the resonators studied by Roszhart. The cantilevers studied by Roszhart are being limited by TED. The thermoelastically forbidden region is where the cantilever Q's would be limited by TED and, therefore, have Q's that fall upon the TED curve.

the thickness of the cantilever. TED is maximized at $f = F_0$. In terms of material properties, F_0 is expressed as

$$F_0 = \frac{\pi \kappa}{2 \rho C_p t^2} \tag{20}$$

where κ is the cantilever material thermal conductivity and t is the cantilever thickness. Using the parameters in Table I, F_0 for 600-Å-thick single-crystal silicon cantilevers is 40 GHz, while 2.3-μm-thick silicon–nitride cantilevers have a characteristic frequency of 390 kHz. We would, therefore, expect to see the effect of TED in 2.3-μm-thick cantilevers that have resonance frequencies in the hundreds of kilohertz range.

Fig. 12 shows a plot of Q_{TED} versus relative frequency ratio f/F_0 for single-crystal silicon at 300K. Q values greater than Q_{TED} are forbidden, as they would be limited by TED. Four sets of data are shown in Fig. 12. The first is data from the work of Roszhart, showing the excellent agreement between theory and the measured Q values of his 10–17.5-μm-thick cantilevers. Also shown are the Q values for 600-Å-thick ($F_0 =$ 40 GHz), 1700-Å-thick ($F_0 = 5$ GHz), and 2400-Å-thick ($F_0 =$ 2.5 GHz) single-crystal silicon cantilevers. Having a relative frequency ratio of 10^{-7} to 10^{-5}, these ultrathin silicon cantilevers are not being limited by TED. Q_{TED} for these cantilevers is in the range of 10^9–10^{11}. The measured Q's of 10^4 are orders of magnitude below the thermoelastic Q limit. In order for 1700-Å-thick silicon cantilevers at 300K to become thermoelastically limited, their relative frequency ratio would need to increase by six orders of magnitude (i.e., their lengths must decrease by three orders of magnitude.) This would result in cantilevers with lengths of only ~ 3 μm. It can, therefore, be safely concluded that, except under extreme design conditions, 600-, 1700-, and 2400-Å-thick single-crystal silicon cantilevers will not have thermoelastically limited Q's.

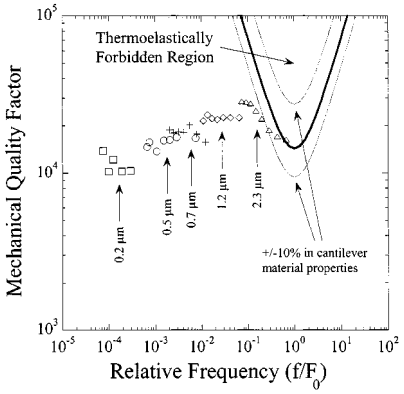

Fig. 13. Plot of measured Q versus relative frequency ratio f/F_0 for silicon–nitride cantilevers. Data for five different silicon–nitride thicknesses are shown. The thickest, i.e., $t = 2.3$ μm, cantilevers are approaching the thermoelastically limited Q values.

The same analysis can be performed for thin silicon–nitride cantilevers. Fig. 13 shows a plot of Q versus f/F_0 for the silicon–nitride cantilevers used in this study. The last set of cantilevers, i.e., $t = 2.3$ μm, are approaching the thermoelastically forbidden region. Two additional curves are shown in Fig. 13. They represent a conservative 10% variation in the material properties used in the calculation of room-temperature TED for silicon–nitride cantilevers. Notice that the 2.3-μm-thick cantilevers have Q's that are decreasing with increasing relative frequency—suggesting that the transition from surface-dominated loss to thermoelastically dominated loss occurs at $f/F_0 \sim 10^{-1}$ for silicon–nitride cantilevers at room temperature. This is the point at which the surface-limited Q equals the thermoelastically limited Q.

VIII. LOSS PARAMETER

In order to make quantitative comparisons of different cantilever geometries and materials, a parameter that we shall call the "loss parameter" γ must be introduced. Recall from (5) that the strategy to make sensitive force sensing microcantilevers was to make them narrow, thin, and long (small k/ω_0) while maintaining high mechanical Q. This general strategy tells us that Q is not the best parameter to use when comparing different oscillators. Even though millimeter-size silicon oscillators can obtain Q's of 6×10^5 at room temperature [9], the large mass and high spring constant of these oscillators make

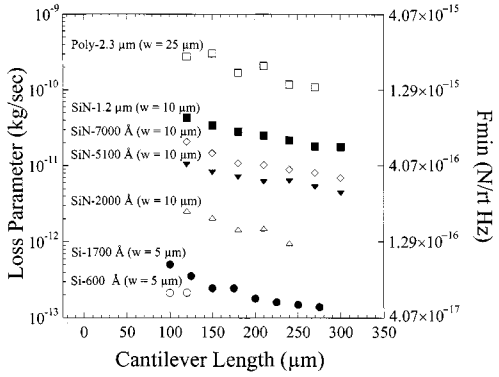

Fig. 14. Loss parameter $\gamma = k/\omega_0 Q$ versus cantilever length comparison plot. Arrays of silicon–nitride, polysilicon, and single-crystal silicon cantilevers are shown with their thicknesses and widths. The equivalent minimum force detectable is shown on the right-hand side for the cantilevers at $T = 300$K.

them poor force detectors. In order to determine whether a cantilever and, more generally, any oscillator, would be a sensitive force measurement device, all of the cantilever dependent terms in (4) must be taken into account. By using $\gamma \equiv k/\omega_0 Q$, we can compare cantilevers of different geometries and materials. In terms of the cantilever geometries and material properties, γ can be expressed as

$$\gamma = 0.246 \frac{wt^2}{lQ} (E\rho)^{1/2} \tag{21}$$

for the first flexural mode of a simple beam cantilever. For more complicated structures, the correct spring constant and resonance frequencies for each mode of oscillation must be used. This analysis can, therefore, be extended to include torsional and double torsional oscillators as well as more complex systems where an effective spring constant and resonance frequency can be either calculated or measured directly.

Fig. 14 shows a summary plot of the loss parameter γ for silicon–nitride, polysilicon, and single-crystal silicon cantilevers. The equivalent minimum force detectable at room temperature is also shown in Fig. 14 for comparison. A 1700-Å-thick single-crystal silicon cantilever of length 275 μm, width 5 μm, and Q of 1.8×10^4 has a loss parameter $\gamma = 1.5 \times 10^{-13}$ kg/s. This corresponds to a room temperature force noise of 5.0×10^{-17} N/$\sqrt{\text{Hz}}$ or 50 aN/$\sqrt{\text{Hz}}$. Let us now compare this cantilever to a thicker silicon–nitride cantilever of approximately the same length. A 5100-Å-thick silicon–nitride cantilever of length 270 μm, width 10 μm, and Q of 1.5×10^4 has a loss parameter $\gamma = 3.3 \times 10^{-12}$ kg/s and a force sensitivity of 233 aN/$\sqrt{\text{Hz}}$. Thus, the silicon cantilever has almost five times lower equivalent force noise than the thicker silicon–nitride cantilever at room temperature even though the Q's are comparable. In Fig. 14, we can also see that the relationship between cantilever stiffness and length causes the longer cantilevers to have better force resolution than the shorter cantilevers. This is expected because longer cantilevers have lower k/ω_0 while having the same approximate Q.

IX. Conclusions

The goal of this paper was to survey the dissipation characteristics of micron- and submicron-thick microcantilevers and to elucidate various dissipation mechanisms. For both silicon–nitride and single-crystal silicon cantilevers, a monotonic reduction in Q with decreasing thickness was observed. This behavior is consistent with surface- dominated energy dissipation. Experiments with 700 °C N_2 and forming gas heat treatments of silicon cantilevers indicated that surface contaminants or defects can be removed via such treatments, allowing significant increase in room temperature Q. Surface effects are also likely to be responsible for the dip in Q observed near 135K in our silicon cantilevers. TED was found to be significant in 2.3-μm-thick silicon nitride cantilevers with frequencies above 50 kHz, but was not significant for any of the thinner cantilevers that we studied.

It is clear that further experiments should be carried out. For example, performing experiments in ultrahigh vacuum would allow better control over surface characteristics and allow the effects due to surface oxidation and contamination to be distinguished. Also, Q measurements over a broader set of cantilever thicknesses need to be performed to more firmly establish the thickness dependence. Finally, the role of other surface characteristics, such as deposited films and surface roughening, should be explored.

Acknowledgment

The authors that H. Jerman for helpful discussions. This work made use of the National Nanofabrication Users Network facilities supported by the National Science Foundation under Award ECS-9731294.

References

[1] T. B. Gabrielson, "Mechanical-thermal noise in micromachined acoustic and vibration sensors," *IEEE Trans. Electron Devices*, vol. 40, pp. 903–909, May 1993.
[2] F. Rief, *Fundamentals of Statistical and Thermal Physics*. New York: McGraw-Hill, 1965.
[3] V. B. Braginsky, *Systems with Small Dissipation*. Chicago, IL: Univ. Chicago Press, 1985.
[4] B. E. White and R. O. Pohl, "Internal friction of subnanometer a-SiO_2 films," *Phys. Rev. Lett.*, vol. 75, no. 24, pp. 4437–4439, 1995.
[5] R. E. Mihailovich and N. C. MacDonald, "Dissipation measurements in vacuum-operated single-crystal silicon microresonators," *Sens. Actuators*, vol. 50, pp. 199–207, 1995.
[6] Y. Jimbo and K. Itao, "Energy loss of a cantilever vibrator" (in Japanese), *J. Horolog. Inst. Japan*, vol. 47, pp. 1–15, 1968.
[7] H. Hosaka, K. Itao, and S. Kuroda, "Damping characteristics of beam-shaped micro-oscillators," *Sens. Actuators*, vol. A49, pp. 87–95, 1995.
[8] A. S. Nowick and B. S. Berry, *Anelastic Relaxation in Crystalline Materials*. New York: Academic, 1972.
[9] R. A. Buser and N. F. De Rooij, "Very high Q-factor resonators in monocrystalline silicon," *Sens. Actuators*, vol. A21–A23, pp. 323–327, 1990.
[10] T. D. Stowe, K. Yasumura, T. W. Kenny, D. Botkin, K. Wago, and D. Rugar, "Attonewton force detection using ultrathin silicon cantilevers," *Appl. Phys. Lett.*, vol. 71, pp. 288–290, 1997.
[11] G. T. Mulhern, D. S. Soane, and R. T. Howe, "Supercritical carbon dioxide drying of microstructures," in *Int. Conf. Solid-State Sens. Actuators Transducers'93*, Yokohama, Japan, pp. 296–299.
[12] D. F. McGuigan, C. C. Lam, R. Q. Gram, A. W. Hoffman, D. H. Douglass, and H. W. Gutche, "Measurements of the mechanical Q of single-crystal silicon at low temperatures," *J. Low Temp. Phys.*, vol. 30, pp. 621–629, 1978.
[13] S. V. Starodubtsev, D. Kaipnazarov, L. P. Khiznichenko, and P. F. Kromer, "Low-temperature internal friction in silicon," *Sov. Phys.—Solid State*, vol. 8, pp. 1521–1524, 1966.

[14] T. D. Stowe, K. Yasumura, T. W. Kenny, D. Botkin, K. Wago, and D. Rugar, "Ultrasensitive vertical force probe for magnetic resonance force microscopy," in *Solid-State Sens. Actuator Workshop*, Hilton Head, SC, 1996, pp. 225–230.
[15] A. N. Cleland and M. L. Roukes, "Fabrication of high frequency nanometer scale mechanical resonators from bulk Si crystals," *Appl. Phys. Lett.*, vol. 69, pp. 2653–2655, 1996.
[16] K. Wago, O. Züger, R. Kendrick, C. S. Yannoni, and D. Rugar, "Low temperature magnetic resonance force detection," *J. Vac. Sci. Technol. B, Microelectron. Process. Phenom.*, vol. 14, no. 2, pp. 1197–1201, 1996.
[17] R. E. Mihailovich, "Low temperature properties of boron doped silicon," *Phys. Rev. Lett.*, vol. 68, pp. 3052–3055, 1992.
[18] C. Zener, "Internal friction in solids I: Theory of internal friction in reeds," *Phys. Rev.*, vol. 52, pp. 230–235, 1937.
[19] ——, "Internal friction in solids II: General theory of thermoelastic internal friction," *Phys. Rev.*, vol. 53, pp. 90–99, 1938.
[20] T. V. Roszhart, "The effect of thermoelastic internal friction on the Q of micromachined silicon resonators," in *Tech. Dig. Solid-State Sens. Actuator Workshop*, Hilton Head, SC, 1990, pp. 13–16.
[21] C. H. Mastrangelo, "Thermophysical properties of low-residual stress, silicon-rich, LPCVD silicon nitride films," *Sens. Actuators*, vol. A21–A23, pp. 856–860, 1990.
[22] J. T. Milek, *Handbook of Electronic Materials 3, Silicon Nitride for Microelectronic Applications, Part 1: Preparation and Properties*. New York: Plenum, 1971, pp. 36–63.
[23] K. E. Petersen, "Silicon as a mechanical material," *Proc. IEEE*, vol. 70, pp. 420–457, May 1982.
[24] Y. S. Touloukian, *Thermophysical Properties of Matter, Vol. 13, Thermal Expansion, Nonmetallic Solids*. New York: Plenum, 1970, p. 154.
[25] ——, *Thermophysical Properties of Matter, Vol. 4, Specific Heat, Nonmetallic Solids*. New York: Plenum, 1970, p. 204.
[26] ——, *Thermophysical Properties of Matter, Vol. 1, Thermal Conductivity, Metallic Elements and Alloys*. New York: Plenum, p. 326.

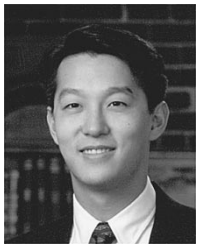

Kevin Y. Yasumura received the B.A. degree in physics from the University of California at Berkeley, in 1994, and the M.S. degree in applied physics from Stanford University, Stanford, CA, in 1998, and is currently working toward the Ph.D. degree at Stanford University. His doctoral work involves studying mechanical energy dissipation in microcantilever oscillators and the application of these oscillators to the detection of small forces.

Timothy D. Stowe received the B.S. degree in applied and engineering physics from Cornell University, Ithaca, NY, in 1993 the M.S. degree in applied physics from Stanford University, Stanford, CA, in 1996, and is currently working toward the Ph.D. degree at Stanford University. His doctoral work involves dissipation force microscopy in regards to external tip-sample dissipation.

Mr. Stowe is a John and Fannie Hertz Fellow.

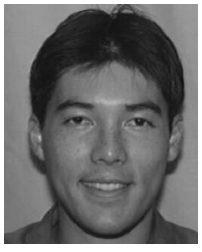

Eugene M. Chow received the B.S. degree in engineering physics from the University of California at Berkeley, in 1995, the M.S. degree in electrical engineering from Stanford University, Stanford, CA, in 1997, and is currently working toward the Ph.D. degree in electrical engineering at Stanford University.

His research interests are in the fabrication, application, and design of microfabricated sensors, with particular interest in scanning probes and through-wafer interconnects.

Timothy Pfafman received the B.S. degree in mathematics and physics from the Massachusetts Institute of Technology, Cambridge, in 1986, and the Ph.D. degree in physics from the University of California at Berkeley, in 1991.

In 1991, he was with the Los Alamos National Laboratory, where he was involved with calorimetric X-ray detectors for astrophysics applications. In 1996, he joined the Design Division, Department of Mechanical Engineering, Stanford University, Stanford, CA, as a Research Associate, where he was involved with general micromachining, sensor development for small satellites, software tools for micromachining, and ultimate frisbee. He is currently a software and hardware consultant in Silicon Valley.

Thomas W. Kenny received the B.S. degree in physics from the University of Minnesota at Minneapolis–St. Paul, in 1983, and the M.S. and Ph.D. degrees in physics from the University of California at Berkeley, in 1987 and 1989, respectively.

He was with the Jet Propulsion Laboratory, where his research focused on the development of electron-tunneling-based high-resolution microsensors. Since 1994, he has been an Assistant Professor with the Mechanical Engineering Department, Stanford University, Stanford, CA. He currently oversees graduate students in the Stanford Microstructures and Sensors Laboratory, whose research activities cover a variety of areas such as advanced tunneling sensors, piezoresistive sensors, cantilever arrays, fracture in silicon, and the mechanical properties of biomolecules and cells. This group is also collaborating with researchers from the IBM Almaden and Zürich Research Centers on nuclear magnetic resonance microscopy as well as AFM thermomechanical data storage.

Dr. Kenny is a Terman Fellow.

Barry C. Stipe received the B.S. degree in physics from the California Institute of Technology, Pasadena, in 1991, and the Ph.D. degree in physics from Cornell University, Ithaca, NY, in 1998. For his doctoral thesis, he combined low-temperature scanning tunneling microscopy (STM) with vibrational spectroscopy, which included the imaging, excitation, manipulation, and spectroscopic characterization of individual chemical bonds within single adsorbed molecules using inelastic tunneling electrons.

His research interests include the study of matter at the atomic and molecular level with the use of proximal probe techniques combined with high-resolution spectroscopies. Since August 1998, he has been with the IBM Research Division, Almaden Research Center, San Jose, CA, with the aim of imaging and studying individual spins with atomic resolution by magnetic resonance force microscopy.

Daniel Rugar (M'87) received the B.A. degree in applied physics (*magna cum laude*) from Pomona College, Pomona, CA, in 1975, and the Ph.D. degree in applied physics from Stanford University, Stanford, CA, in 1982.

From 1982 to 1984, he was the Hunt Fellow of the Acoustical Society of America and a Research Associate at Stanford University, where he was involved with acoustic microscopy and phonon dispersion in superfluid helium. In 1984, he joined the IBM Research Division, Almaden Research Center, San Jose, CA, where he is currently Manager of nanoscale studies. He has published over 80 papers and holds 13 patents. He has worked on many aspects of high-density data storage and scanning probe microscopy, and his current research interests include new techniques for ultrahigh density data storage, magnetic resonance force microscopy, and ultrasensitive force detection.

Dr. Rugar is a member of the American Physical Society and currently serves as a distinguished lecturer for the IEEE Magnetics Society.